

# NOISE 2 imaging system: seeing through scattering tissue with a reference point

David Abookasis and Joseph Rosen

Department of Electrical and Computer Engineering, Ben-Gurion University of the Negev,  
P.O. Box 653, Beer-Sheva 84105, Israel

Received October 4, 2003

We propose a fly-eye-like imaging system for seeing objects embedded in scattering media. Objects are recovered from many speckled images observed by a digital camera through a microlens array. Each microlens in the array generates a speckle image of the object buried between two layers of chicken breast tissue. In the computer each image is Fourier transformed jointly with an image of the speckled pointlike source captured under the same conditions. A set of the squared magnitudes of the Fourier-transformed pictures is accumulated to form a single average picture. This final picture is again Fourier transformed, resulting in the reconstruction of the hidden object. © 2004 Optical Society of America

OCIS codes: 030.6140, 030.6600, 170.1650, 170.3010, 170.3880.

During the past decade, optical imaging through scattering media has proved to be an effective medical diagnostic because it is safe, noninvasive, and lower in cost than conventional radiation techniques. Many optical techniques for imaging through diffusing tissues have been proposed,<sup>1</sup> despite the strong attenuation and scattering of light caused by tissue constituents. Each of these technologies has particular advantages, but some of them are complicated and expensive.

We recently reported on a new method of imaging through a scattering medium, based on a space-time analogy with speckle interferometry,<sup>2,3</sup> termed noninvasive optical imaging by a speckle ensemble<sup>4</sup> (NOISE). The setup, shown in Fig. 1, averages over many projections of speckled images to recover the shapes of hidden objects in a scattering medium. This laser-illuminated system contains a microlens array (MLA) that images many speckle pictures of the embedded object through different parts of the scattering medium. The speckled images from the entire array are imaged onto a CCD by an imaging lens and then digitally processed in the computer by an algorithm that resembles the shift-and-add algorithm.<sup>3</sup> Each image is shifted to a common center, and then all centered images are accumulated into a single average picture. By this technique we have successfully recovered, separately, transparent and opaque objects from a set of many degraded images.<sup>4</sup> However, the process of shifting the images to a common center is not completely accurate and therefore reduces the overall resolution of the system.

In this Letter we report on a different NOISE algorithm, NOISE 2, for recovering embedded objects. In contrast to our previous algorithm, this time there is no need to shift the speckled images toward a common center. The algorithm makes use of the point-source reference idea.<sup>5</sup> In addition to the speckled images of the object, we record speckled images of a pointlike object. After collecting all the object's speckled images by using the MLA, we use the point source to illuminate the setup, and speckled patterns of this point source, through the same number of channels, are

captured by a CCD. Each subimage of the speckled object is placed side by side in the computer with a corresponding subimage of the speckled pointlike source, and the two images are jointly Fourier transformed. The squared magnitudes of the jointly transformed pictures are accumulated to compose a single average joint power spectrum. Object reconstruction is achieved by another Fourier transform (FT) of this average spectrum. As a result, the final image is close to a cross correlation between the object function and a narrow pointlike source. The main idea of this technique is that the relative locations between the speckle patterns do not have any influence on the result of the reconstruction. The method is based on the assumption that, in every channel, the object and the pointlike reference suffer from the same scattering. Therefore they are both shifted by the same amount relative to other channels, but the mutual distances between the speckled images of the object and the pointlike reference in the entire channels are the same.

It is assumed that the exposed object (without scattering medium  $T_2$  in front of it) seems approximately the same for each microlens. Let the function  $f_k(x, y)$  represent the intensity of the  $k$ th speckled image of the same embedded object function  $s(x, y)$ . Function  $r_k(x, y)$  stands for the  $k$ th intensity of the speckled image of the pointlike function approximated by Dirac

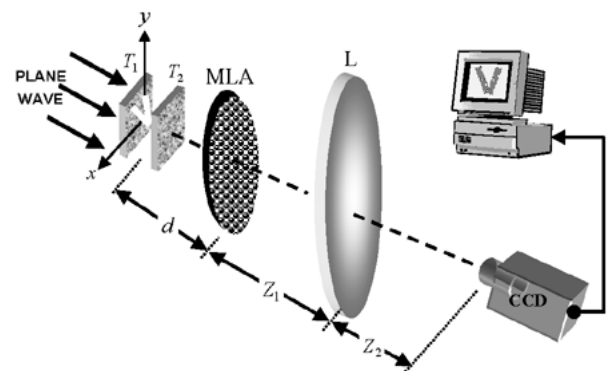


Fig. 1. Schematic of the NOISE system.

delta function  $\delta(x, y)$ . Under coherent illumination, both functions  $s(x, y)$  and  $\delta(x, y)$  are convolved with a randomly speckled  $k$ th point-spread function (PSF),  $h_k(x, y)$ , as follows:

$$\begin{aligned} f_k(x, y) &= |s(x, y) * h_k(x, y)|^2, \\ r_k(x, y) &\equiv |\delta(x, y) * h_k(x, y)|^2 = |h_k(x, y)|^2, \\ k &= 1, 2, \dots, K, \end{aligned} \quad (1)$$

where the asterisk stands for the operation of two-dimensional convolution and  $K$  is the total number of imaging channels. It is assumed that the scattering layer induces in each channel a random PSF  $h_k(x, y)$  that satisfies the relation that the ensemble average over the entire array is

$$\frac{1}{K} \sum_k h_k(x, y) \equiv h_0(x, y), \quad (2)$$

where  $h_0(x, y)$  is the diffraction-limited PSF in each channel, without the presence of scattering layer  $T_2$ .

In the computer the reference and the object speckled images are combined such that both are situated in the same plane, separated by a distance  $(a, b)$  from each other. The accumulated intensity pattern of the entire  $K$  joint power spectrum is

$$\begin{aligned} I(u, v) &= \frac{1}{K} \sum_k I_k(u, v) \\ &= \frac{1}{K} \sum_k [|\widehat{\mathfrak{F}}_{2D}[f_k(x + x_k + a/2, y + y_k + b/2) \\ &\quad + r_k(x + x_k - a/2, y + y_k - b/2)]|^2 \\ &\approx \frac{1}{K} \sum_k |F_k(u, v)|^2 + |R_k(u, v)|^2 \\ &\quad + F_k^*(u, v)R_k(u, v)\exp[-i2\pi(au + bv)] \\ &\quad + F_k(u, v)R_k^*(u, v)\exp[i2\pi(au + bv)], \end{aligned} \quad (3)$$

where  $u$  and  $v$  are the spatial frequency coordinates;  $\widehat{\mathfrak{F}}_{2D}$  denotes a two-dimensional FT operation; a superscript asterisk denotes a complex conjugate;  $F_k$  and  $R_k$  are the FTs of  $f_k$  and  $r_k$ , respectively; and  $(x_k, y_k)$  is the  $k$ th random shift that results from propagation of light through the  $k$ th portion of the scattering layer. Inasmuch as the light from the reference and the object suffers from the same scattering in each channel, it is shifted by the same distance in each  $k$ th channel. Therefore the magnitude expression in Eq. (3) eliminates the linear phase factor that results from the shift  $(x_k, y_k)$ . Another FT of the expression of Eq. (3) yields the output function

$$\begin{aligned} C_{\text{out}}(\xi, \eta) &= \frac{1}{K} \sum_k [f_k(\xi, \eta) \otimes f_k(\xi, \eta) \\ &\quad + r_k(\xi, \eta) \otimes r_k(\xi, \eta)] \\ &\quad + \left[ \frac{1}{K} \sum_k r_k(\xi, \eta) \otimes f_k(\xi, \eta) \right] * \delta(\xi - a, \eta - b) \\ &\quad + \left[ \frac{1}{K} \sum_k f_k(\xi, \eta) \otimes r_k(\xi, \eta) \right] * \delta(\xi + a, \eta + b), \end{aligned} \quad (4)$$

where  $(\xi, \eta)$  are the coordinates of the output plane and  $\otimes$  denotes correlation. It is clear from Eq. (4) that three spatially separated Fourier orders can be observed. The second and the third terms at points  $(\pm a, \pm b)$  are of interest here; they correspond to the convolution between object  $s(\xi, \eta)$  with narrow functions, as discussed below. Therefore one retrieves the object image by observing the pattern at the vicinity of the points  $(a, b)$  or  $(-a, -b)$ .

We concentrate now only on the last term in Eq. (4), which is expected to yield the reconstructed image at point  $(a, b)$ . Substituting expressions (1) and (2) into the third term of Eq. (4) and following a straightforward algebra yield for the third term, we obtain

$$\begin{aligned} C_3(\xi - a, \eta - b) &= \frac{1}{K} \sum_k |s(\xi, \eta) * h_k(\xi, \eta)|^2 \\ &\quad \otimes |h_k(\xi, \eta)|^2 \\ &\equiv |s(\xi, \eta) * h_0(\xi, \eta)|^2 \otimes |h_0(\xi, \eta)|^2 \\ &\quad + \sigma^2(\xi, \eta) * |s(\xi, \eta)|^2 \otimes |h_0(\xi, \eta)|^2 \\ &\quad + \sigma^2(\xi, \eta) \otimes [|s(\xi, \eta) * h_0(\xi, \eta)|^2 \\ &\quad + |s(\xi, \eta)|^2 * \sigma^2(\xi, \eta)]. \end{aligned} \quad (5)$$

The first term of expression (5) is the desired image of the embedded object. As can be seen from this term, one obtains the image by convolving object function  $s(\xi, \eta)$  twice with the diffraction-limited PSF  $h_0(\xi, \eta)$ . Therefore, independently of the scattering, this imaging method has an inherent loss of resolution because of the double convolution with the PSF  $h_0(\xi, \eta)$ . The rest of the terms of expression (5) are convolution between the object and the variance function  $\sigma^2(\xi, \eta)$ , defined as  $\sigma^2 = (1/K) \sum_k |h_k - h_0|^2$ . Clearly  $\sigma^2(\xi, \eta)$  is wider than  $h_0(\xi, \eta)$  because the scattering layer broadens the diffraction-limited image of a point. Therefore we conclude that the terms of convolution with the variance function in expression (5) blur the diffraction-limited image of the object. The value of these blurring terms is determined by the average value of the variance  $\sigma^2(\xi, \eta)$ .

The NOISE system shown in Fig. 1, with the method of point-source reference described above, was experimentally tested. A transparent object in the form of the letter V with a size of  $7 \times 11$  mm was embedded between two layers of chicken breast tissue separated from each other by a distance of 12 mm. The thicknesses of the layers, back  $T_1$  and front  $T_2$ , were  $\sim 3$  and  $\sim 4$  mm, respectively. The scattering coefficient value of the layers is the same as in Ref. 4. Rear tissue  $T_1$  was illuminated by the collimated beam of a 35-mW He-Ne laser with 632.8-nm wavelength. Speckle images were taken with the MLA placed a distance  $d = 160$  mm from the object. We used  $12 \times 11 = 132$  hexagonal refractive microlenses from the MLA in the experiment. The radius of each microlens was  $r_l = 250 \mu\text{m}$ , and its focal length was 3.3 mm. Under these conditions the optical system without the tissues can resolve a minimum size of  $\lambda d/r_l \equiv 0.4$  mm. The MLA image plane is then imaged by a single spherical lens, L,

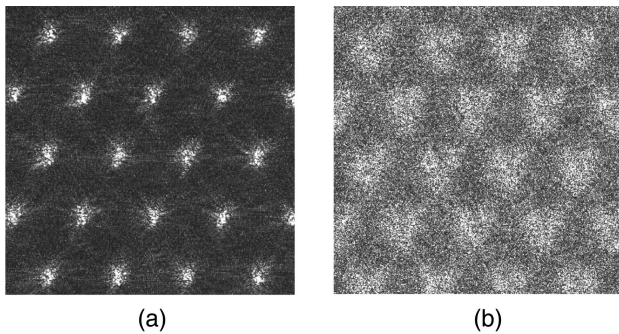


Fig. 2. Twenty-two projections, of 132 speckled images, of (a) the point-source reference and (b) the object.

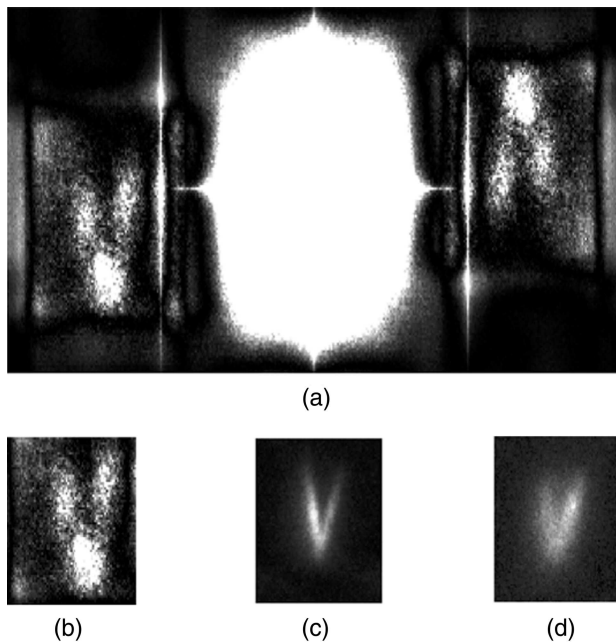


Fig. 3. (a) Experimental results of the NOISE system. The desired image of the observed object is recovered on both sidelobes. (b) Left sidelobe from (a). (c) Average picture of the entire array when the letter V is positioned in front of layer  $T_1$  and layer  $T_2$  is removed. (d) Recovered image of the letter V obtained by our previous algorithm.<sup>4</sup>

onto a CCD camera. The spherical lens with 300-mm focal length matches the MLA image plane onto the CCD. Figure 2 shows several elemental images from among 132 speckled images of the point-source [Fig. 2(a)] and of the object [Fig. 2(b)], as recorded by the CCD.

In the computer each subimage of the array that originates from the object is combined with the corresponding subimage of the array that originates from the point source. We create the point source by placing a pinhole attached to tissue  $T_1$  from the side illuminated by the laser. The pinhole is located a short distance behind layer  $T_1$  and the object, which enables us to neglect the mutual movement between the point and the object along the full angular range of  $\sim 2^\circ$  of the MLA. Thus from a practical point of view the

point source and the object are considered to reside at the same location in space. The light from the pinhole goes through the object such that the embedded object does not need to be removed. Although this method becomes more complicated as a result of the double recording process, the increase of accuracy justifies its use. Each enlarged input plane, which contains the speckled point source beside the speckled object, is Fourier transformed. The squared magnitude of each channel's spectrum is accumulated with all the others. This average joint power spectrum is then Fourier transformed again to the output correlation plane. The three orders of the correlation plane that contains the revealed image of the object in two sidelobes are clearly shown in Fig. 3(a). Figure 3(b) shows the recovered image of the letter V taken from the left sidelobe of Fig. 3(a). For comparison, Fig. 3(c) shows the average image of the letter V without scattering layer  $T_2$ . The effect of extending the object in Fig. 3(b) in comparison to Fig. 3(c) can be clearly seen. This phenomenon is due to the double convolution with the PSF  $h_0$  in Fig. 3(b), in contrast to a single convolution in Fig. 3(c). The image obtained by use of our version of the shift-and-add algorithm<sup>4</sup> is depicted in Fig. 3(d). From comparison of Figs. 3(b) and 3(d) it seems that imaging by cross correlation with a point reference [Fig. 3(b)] yields better resolution than imaging by the add-and-shift algorithm [Fig. 3(d)]. The improvement in resolution is quantified by comparison of the depth of the notch between the sides of the letter V in the results. Our measurements indicate that the notch in Fig. 3(b) is, on average, 30% deeper than the notch in Fig. 3(d).

In conclusion, we have proposed an alternative reconstruction algorithm for the recently proposed NOISE system. This algorithm obviates the need to shift every speckled pattern of the object to an estimated, and inaccurate, common center. Thus, one source of resolution reduction is eliminated by this algorithm. However, this method produces another source of low resolution because the output image is obtained as a double convolution of the object with the PSF of a single channel.

Because the proposed method provides the advantages of simple design and real-time image reconstruction, it might be useful in several imaging applications, especially in real-time medical diagnostics.

This research was supported by Israel Science Foundation grant 119/03. J. Rosen's e-mail address is rosen@ee.bgu.ac.il.

## References

1. J. C. Hebden, S. R. Arridge, and D. T. Delpy, *Phys. Med. Biol.* **42**, 825 (1997).
2. A. Labeyrie, *Astron. Astrophys.* **6**, 85 (1970).
3. R. H. T. Bates and F. M. Cady, *Opt. Commun.* **32**, 365 (1980).
4. J. Rosen and D. Abookasis, *Opt. Lett.* **29**, 253 (2004).
5. C. Y. C. Liu and A. W. Lohmann, *Opt. Commun.* **8**, 372 (1973).